SCIENCE CHINA
Information Sciences

• RESEARCH PAPER •

April 2020, Vol. 63 140902:1–140902:13
https://doi.org/10.1007/s11432-019-2809-3

Special Focus on Exploring the Far Side of the Moon — the Preliminary Data From Chang'e-4 Mission

Petrography and chronology of lunar meteorite Northwest Africa 6950

Zemin BAO[1], Yuruo SHI[1*], J. Lawford ANDERSON[2], Allen KENNEDY[3], Zuokai KE[4], Xiangping GU[4], Peizhi WANG[1], Xiaochao CHE[1], Yuelan KANG[1], Huiyi SUN[1] & Chen WANG[1]

[1]*Beijing SHRIMP Center, Institute of Geology, Chinese Academy of Geological Sciences, Beijing* 100037*, China;*
[2]*Department of Earth and Environment, Boston University, Boston* MA 02215*, USA;*
[3]*John de Laeter Centre, Curtin University, Perth* WA 6845*, Australia;*
[4]*School of Geosciences and Infophysics, Central South University, Changsha* 410083*, China*

Received 3 June 2019/Revised 2 October 2019/Accepted 19 January 2020/Published online 9 March 2020

Abstract Northwest Africa (NWA) 6950 is an olivine-gabbro lunar meteorite that has a distinctly different petrographic texture from other lunar basalts. In this contribution, we report the petrography, mineralogy, and U-Pb geochronology of baddeleyite and phosphate in this lunar meteorite and make a comparison with other NWA 773 paired meteorites. NWA 6950 consists mainly of coarse-grained olivine, pyroxene, and plagioclase, with minor ilmenite, chromite, troilite, baddeleyite, taenite, and apatite. The abundant rounded to euhedral olivine has a limited Fo ranging from 68 to 69. Pyroxenes include both augite and pigeonite, with a narrow range of Mg#=71–80, and composition, respectively, $En_{46\text{-}52}Fs_{12\text{-}16}Wo_{32\text{-}41}$ and $En_{58\text{-}68}Fs_{19\text{-}28}Wo_{7\text{-}20}$. Plagioclase is mainly anhedral, conforming to the crystal margins of olivine and pyroxene. The plagioclase grains are elongated and several hundreds of microns in length. Raman spectra shows that plagioclase has been transformed into maskelynite, which is very calcic ($An_{87\text{-}95}$) with low sodium and very low potassium ($Ab_{4\text{-}9}Or_{0.6\text{-}3.7}$). The weighted mean $^{207}Pb/^{206}Pb$ ages of baddeleyite and phosphate measured using a sensitive high resolution ion micro probe (SHRIMP II) are 3119 ± 16 Ma ($n = 9$, MSWD = 2.5) (mean squared weighted deviates, MSWD) and 3119 ± 18 Ma ($n = 15$, MSWD = 2.1), respectively, giving the crystallization age of the meteorite. NWA 6950 has similar mineral compositions, geochemical characteristics, and an almost identical age of crystallization to the magnesian gabbro of the NWA 773 clan. We conclude that NWA 6950 and NWA 773 are paired meteorites, which crystallize at ca. 3119 Ma, and represent magmatic activities in the KREEP (potassium (K), rare earth elements (REE) and phosphorus (P) rich lunar material) region of the Moon.

Keywords Northwest Africa 6950, lunar meteorite, U-Pb chronology, baddeleyite, phosphate

Citation Bao Z M, Shi Y R, Anderson J L, et al. Petrography and chronology of lunar meteorite Northwest Africa 6950. Sci China Inf Sci, 2020, 63(4): 140902, https://doi.org/10.1007/s11432-019-2809-3

1 Introduction

The rocks from the Apollo and Luna missions have provided opportunities to study the formation and evolution of the Moon, but they represent only a small portion of the Lunar surface [1]. Lunar meteorites represent a possibly broader random sampling of the Moon and provide complementary information on the nature of the Moon and its evolutionary history [2, 3].

Northwest Africa (NWA) 6950 is a 1649 g lunar meteorite, whose lithology is magnesian gabbro with thin black shock veins. It is inferred to be paired with other lunar meteorites called the NWA 773

* Corresponding author (email: shiyuruo@bjshrimp.cn)

clan [4, 5], which is a group of paired or petrogenetically related stones that include NWA 773, NWA 2977, NWA 2700, NWA 2727, NWA 3160, NWA 7007, and etc. [6–12]. In recent years, NWA 773 and its paired meteorites have received extensive attention from planetary chemists because they are significantly different from Apollo and Luna samples and other lunar meteorites [13]. Scientists studying the Apollo and Luna samples, generally conclude that the volcanic eruption of the mare basalts lasts from 3900 Ma to ∼3150 Ma, after which there is no large-scale volcanic activity [5,14–16]. However, in recent years, studies on the age of crystallization of lunar meteorites have modified this conclusion [17–19]. The NWA 773 clan is 30–40 Ma younger than the youngest Apollo samples (about ∼3.16 Ga, 12051 and 12065 samples [5,15]), and provides new opportunities to study the formation and evolution of lunar magmas [20–23]. Moreover, compared to other younger lunar meteorites such as LAP 02205/NWA 4734, the gabbro clast of NWA 773 has unique geochemical characteristics including KREEP-like rare earth element (REE) patterns, but at lower concentrations [13]. Based on petrological and mineralogical investigation of another NWA 773 paired meteorite, NWA 2977, Nyquist et al. [24] suggested that the meteorite probably originates from a KREEP-rich source. The study by Zhang et al. [25] suggests that the KREEP-like REE pattern of NWA 2977 is likely owing to the addition of a KREEP component rather than small degrees of partial melting [26]. The parental magma of NWA 2977 might have obtained its KREEP-like REE features in a magma chamber deep in the Lunar mantle. However, the magmatic evolution revealed by the NWA 773 clan of meteorites has not been completely explained and further investigation is needed.

NWA 6950 is considered to be a member of the NWA 773 paired meteorites. However, in contrast to the other members, research on NWA 6950 was only carried out by Shaulis et al. [4], who obtained a Pb-Pb age (3100 ± 16 Ma, LA-ICP-MS) from 7 analyses on 4 baddeleyite grains. Additionally, petrological study of NWA 6950 is very limited. Here, we describe the petrography of NWA 6950 and present the $^{207}Pb/^{206}Pb$ ages of baddeleyite and phosphate. Moreover we compare the meteorite with NWA 773, examine the evolutionary connection between them, and measure their crystallization age more accurately.

2 Analytical methods

2.1 Sample

The NWA 6950, which was found near the border between Mali and Algeria in 2011, is a single yellowish-green stone (1649 g, broken into 8 pieces) with a partial fusion crust. It is a lunar gabbro with thin black shock veins that can be seen in the interior of the meteorite. The stone is relatively coarse grained with a cumulate igneous texture (Figure 1). Major minerals are olivine, pigeonite, and subcalcic augite, with interstitial calcic plagioclase. Accessory minerals include apatite, ilmenite, Ti-chromite, armalcolite, troilite, baddeleyite, taenite and merrillite [27]. Our sample of NWA 6950 is cut into three thin slices and embedded in epoxy resin mounts, which are polished to provide a flat surface for analysis. The mount size is φ25 mm × 7 mm. Before microprobe *in-situ* analysis, the mount surface is gold-plated or carbon-coated.

2.2 Petrography and mineralogy

The petrography of NWA 6950 is studied using a CARLZEISS MERLIN compact scanning electron microscope (SEM) and backscattered electron (BSE) microscope with imaging at the Beijing SHRIMP Center, Institute of Geology, Chinese Academy of Geological Sciences. The mineral elemental mapping and identification are made using Oxford IE 250 energy dispersive spectroscopy (EDS) system. Elemental mapping is done at a 20 kV accelerating voltage with a 20 nA beam current. Surface quantitative analysis of major and accessory minerals is carried out in order to find the exact location of baddeleyite and phosphate grains.

Mineral compositions are measured with the SHIMADZU EPMA 1720 electron microprobe at Central South University (China). Natural and synthetic standards are used and all data are corrected by the ZAF method. Silicate mineral quantitative analyses are performed using a 15 kV accelerating voltage,

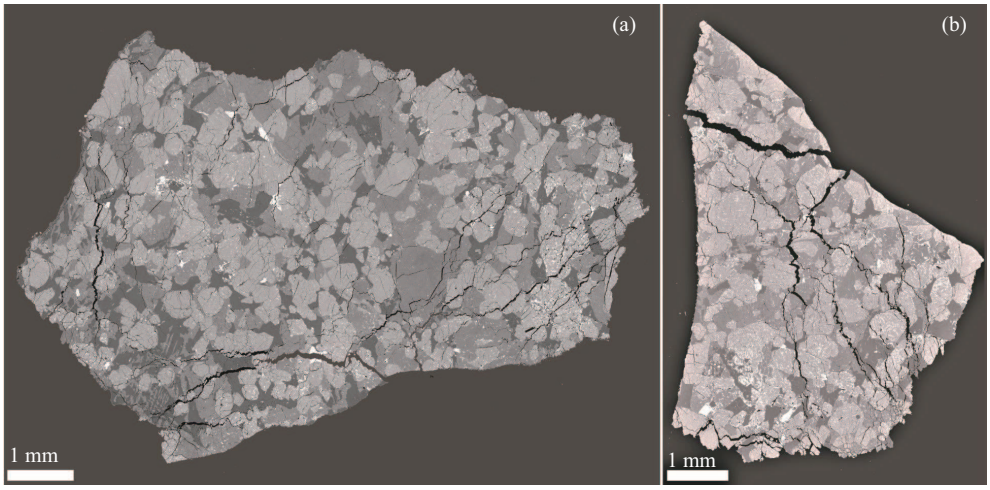

Figure 1 The BSE image of Northwest Africa (NWA) 6950.

10 nA beam current, and a 5 μm beam size. Phosphate minerals (apatite and merrillite) analyses employ a 15 kV accelerating voltage, 10 nA beam current, and a 1 μm beam size.

2.3 U-Pb chronology

The U-bearing accessory minerals in NWA 6950 are mainly baddeleyite and Ca-phosphate, which are distributed among plagioclase, olivine and ilmenite. U-Pb dating analysis is performed on a sensitive high resolution ion micro probe at the Beijing SHRIMP Center, Institute of Geology, Chinese Academy of Geological Sciences. An O_2^- primary ion beam of 1.4 nA is accelerated to 10 keV energy. In order to increase the stability of the dating, a Kohler focusing mode is used to obtain a uniform-density beam size of 10–12 μm. Secondary ions of $^{196}Zr_2O^+$ (for baddeleyite), $^{175}Ca_2PO_4^+$ (for phosphate), $^{204}Pb^+$, background, $^{206}Pb^+$,$^{207}Pb^+$,$^{208}Pb^+$,$^{238}U^+$,$^{248}ThO^+$ and $^{254}UO^+$ are pulse counted on an electron multiplier (EM) with counting time between 1–30 s. In order to minimize possible surface contamination (most likely from the sample polishing and cleaning process, as well as the gold coating), each analysis is pre-sputtered for 3 min using a 50 μm ×50 μm raster.

Phalaborwa baddeleyite (2059.6 ± 0.35 Ma, [28]) is used as the external calibration standard for baddeleyite analysis. Baddeleyite data is processed according to the method of Williams [29]. Because all the phosphates for chronology in NWA 6950 are apatite and merrillite, the NW-1 apatite is used for dating (1160 ± 5 Ma, [30]) and Durango is used for U concentration ($U = 9$ ppm, [31]) as the calibration standards. Phosphate age data processing is performed following the method of Nemchin et al. [32] and Sano et al. [33], while U, Th concentrations are calculated by the method of [30].

3 Results

3.1 Petrography and mineralogy

NWA 6950 has a typical gabbro texture and is predominantly composed of coarse-grained olivine, pyroxene and plagioclase, with minor ilmenite, chromite, troilite, baddeleyite, taenite, apatite and merrillite (Figure 2(a) and (b)). The olivine grains form a cumulate texture with interstices filled by irregular pyroxene grains or occur within poikilitic pyroxene grains. Ruzicka et al. [27] revealed that low-Ca pyroxene, pigeonite, and subcalcic augite exist with plagioclase that is high in calcium and low in potassium ($An_{87.9\text{-}93.0}Or_{1.1\text{-}0.9}$). The BSE images (Figure 2(c)) show that in NWA 6950 there are some mineralogical features indicative of shock metamorphism. A few thin shock-induced melt veins and melt pockets occur mainly in pyroxene grains and in small olivine fragments.

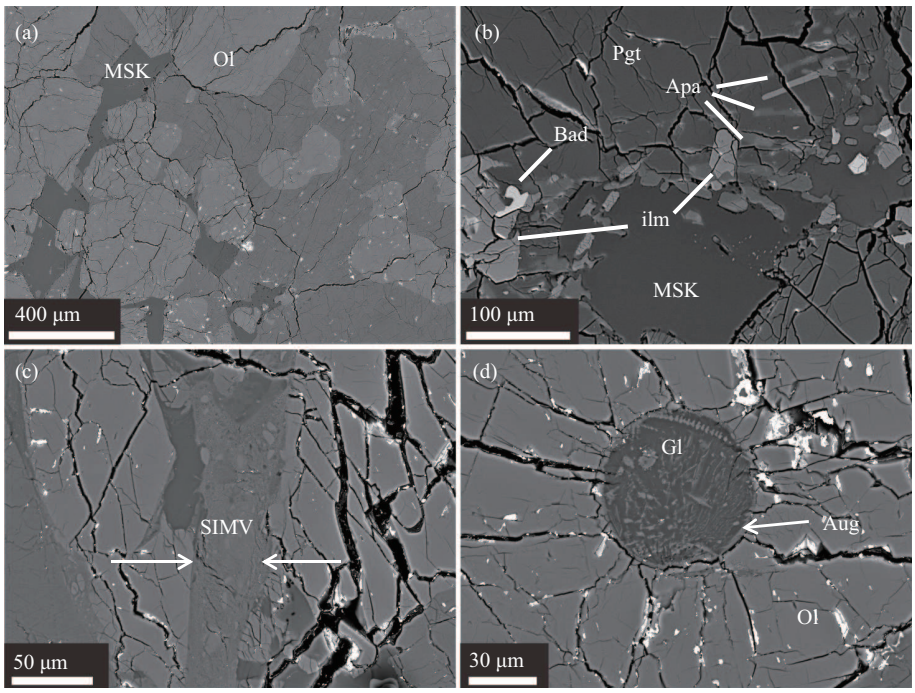

Figure 2 The BSE images of representative areas in NWA 6950. (a) Local details of the rock; (b) morphology of some accessory minerals in the rock; (c) a SIMV-shock induced melt vein in the stone; (d) volcanic glass. Ol: olivine, Pgt: pigeonite, MSK: maskelynite, Apa: apatite, Bad: baddeleyite, ilm: ilmenite, Gl: glass.

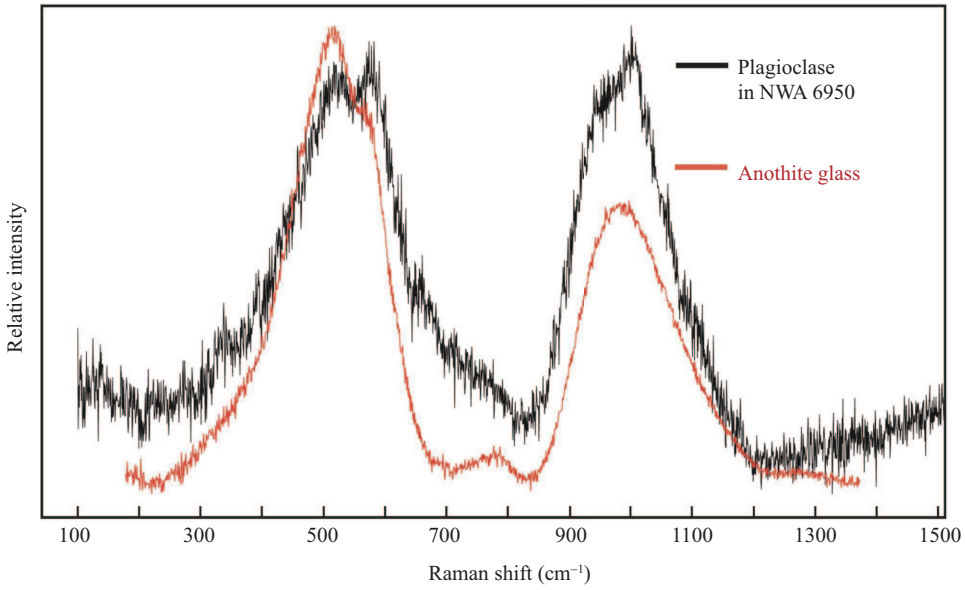

Figure 3 Raman spectra of plagioclase in NWA 6950.

The high abundance of olivine in NWA 6950 and the rounded to euhedral shapes indicate that olivine is the first phase to crystallize. Olivine has a very limited Mg# value range from 68 to 69. MnO content varies from 0.28 wt.% to 0.36 wt.%, and the CaO content has an average value of 0.18 wt.% (Table 1). Several olivines have trapped melt inclusions of glass and other minerals and are rimmed by augite (Figure 2(d)).

Plagioclase is mostly anhedral, conforming to the crystal margins of olivine and pyroxene (Figure 2(a)). Raman spectra show that plagioclase has been transformed into maskelynite [34] (Figure 3). Obvious wide peaks at 517 nm and 980 nm within the Raman spectrum correspond to anorthite glass. Most of the

Table 1 Composition of major elements of representative plagioclase, olivine and pyroxene grains from NWA 6950 and the comparison with NWA 773 and NWA 2977[a)]

Plagioclase	NWA 6950						NWA 773 [5]		NWA 2977 [25]	
	4-3-P7	4-3-P10	4-4-P11	4-5-P7	5-7-P7	5-9-P6	A1	A3	IP10	IP22
SiO_2	44.27	46.84	47.62	45.04	44.93	45.13	46.29	45.11	45.0	49.4
Al_2O_3	34.50	33.12	32.63	34.36	34.27	34.32	33.66	34.76	35.2	32.3
TiO_2	bd	0.05	0.04	bd	0.05	0.06				0.11
MgO	0.09	0.17	0.13	0.16	0.10	0.11	0.19	0.17	0.08	0.17
Cr_2O_3	bd	0.03	bd	bd	0.01	bd				
CaO	20.14	18.94	18.27	19.86	19.87	19.89	18.29	18.70	19.1	15.7
MnO	bd	0.03	0.02	bd	0.03	0.01				
FeO	0.34	0.2	0.35	0.26	0.21	0.29	0.32	0.29	0.24	0.45
SO_3	bd	bd	bd	0.02	0.03	bd				
Na_2O	0.47	1.03	1.02	0.54	0.60	0.61	0.99	0.76	0.67	1.34
K_2O	0.10	0.19	0.64	0.12	0.15	0.15	0.19	0.18	0.09	1.24
Total	99.91	100.65	100.70	100.36	100.24	100.56	99.95	100.10	100.4	100.7
An	95.4	90.1	87.5	94.7	94.0	93.9	93-97	95-98	93.5	80.1
Ab	4.0	8.9	8.8	4.7	5.1	5.2	3-7	2-5	6.0	12.3
Or	0.6	1.1	3.7	0.7	0.9	0.8			0.5	7.5
Olivine	NWA 6950						NWA 773 [5]		NWA 2977 [25]	
	5-1-P1	5-2-P1	5-6-P6	5-8-P3	5-9-P3	4-3-P2	A1	A3	IP35	
SiO_2	37.50	37.45	37.30	37.22	37.53	38.01	37.65	37.80	38.1	
Al_2O_3	bd	bd	bd	bd	0.02	0.12	0.19	0.06	bd	
TiO_2	0.04	0.06	0.03	0.03	bd	bd	0.04	0.05	0.08	
MgO	33.80	33.74	33.88	34.46	34.24	33.79	34.15	36.21	33.5	
Cr_2O_3	0.06	0.01	0.07	0.05	0.07	0.06	0.06	0.07	0.03	
CaO	0.22	0.17	0.14	0.19	0.18	0.19	0.22	0.17	0.15	
MnO	0.36	0.35	0.28	0.29	0.34	0.33	0.31	0.24	0.24	
FeO	28.18	27.85	27.90	27.90	27.43	27.24	28.30	26.11	27.6	
SO_3	bd	bd	bd	bd	0.06	0.08				
Na_2O	bd	bd	bd	bd	bd	0.01	0.01	0.01	bd	
K_2O	bd	0.02	bd	bd	0.02	bd	0.01	0.01	bd	
Total	100.16	99.65	99.61	100.14	99.87	99.82	100.95	100.77	99.6	
Fo	68	68	68	69	69	69	68	71	68	
Fa	32	32	32	31	31	31	32	29		
Pyroxenes	NWA 6950						NWA 773 [5]		NWA 2977 [25]	
	4-3-Pig, $n = 4$	4-3-Aug, $n = 4$	4-4-Pig, $n = 7$	4-4-Aug, $n = 3$	5-8-Pig, $n = 7$	5-8-Aug, $n = 6$	A1(Pig)	A1(Aug)	IP1(Aug)	IP2(Pig)
SiO_2	54.04	52.68	52.81	52.19	52.92	52.30	52.88	51.77	52.4	53.9
Al_2O_3	0.98	2.56	1.45	2.03	1.06	2.08	1.39	2.28	2.07	1.40
TiO_2	0.40	0.34	0.42	1.10	0.52	0.52	0.40	0.44	0.24	0.17
MgO	23.97	17.71	22.03	16.50	22.92	17.67	22.72	17.45	18.5	24.3
Cr_2O_3	0.48	0.96	0.62	0.77	0.45	0.83	0.53	0.86	1.01	0.73
CaO	4.47	17.78	7.22	18.96	5.25	18.10	5.55	16.81	16.3	5.87
MnO	0.29	0.18	0.29	0.19	0.30	0.19	0.32	0.22	0.18	0.28
FeO	15.69	8.94	15.07	9.42	16.02	8.99	16.28	9.60	9.21	13.9
SO_3	0.01	bd	bd	0.02	bd	0.01				
Na_2O	bd	0.02	0.02	0.04	0.01	0.03	0.02	0.06	0.03	0.00
K_2O	0.01	bd	bd	bd	bd	bd	0.01	0.01		
Total	100.33	101.17	99.93	101.22	99.46	100.71	100.10	99.49	99.9	100.6
Mg#	71-76	77-80	71-76	76-76	71-73	76-80	70-75	73-78	78	76
En	65-68	47-52	58-64	46-47	62-65	46-52	59-66	46-53	52.4	67.2
Fs	22-28	12-16	19-26	15-16	24-27	12-16	22-27	14-18	14.5	21.3
Wo	7-12	32-40	10-20	37-39	9-14	33-41	8-15	31-40	33.1	11.6

a) A1, A3: area of magnesian gabbro lithology in NWA 773; Aug: augite; Pig: pigeonite; bd: below detection limit.

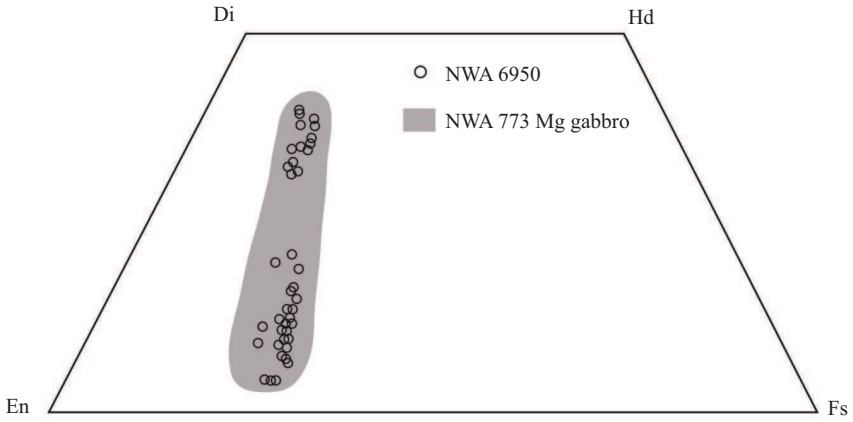

Figure 4 Pyroxene compositions plotted on the pyroxene quadrilateral for different meteorites (data of NWA 773 from [5]).

maskelynite grains are elongated and have a length of several hundred microns. Some plagioclase grains are very calcic ($An_{87\text{-}95}$) and have low sodium and very little potassium ($Ab_{4\text{-}9}Or_{0.6\text{-}3.7}$). Furthermore, the plagioclase has a FeO concentration of 0.25–0.35 wt.% and an average MgO concentration of 0.13 wt.% (Table 1).

Representative chemical compositions of pyroxenes are given in Table 1. The distribution of analysis points in the pyroxene quadrilateral diagram (Figure 4) shows that pyroxene in NWA 6950 includes both augite and pigeonite, with the composition of NWA 6950 pyroxene completely falling within the field of NWA 773 pyroxene. Both augite and pigeonite grains have narrow compositional ranges of $En_{46\text{-}52}Fs_{12\text{-}16}Wo_{32\text{-}41}$ and $En_{58\text{-}68}Fs_{19\text{-}28}Wo_{7\text{-}20}$, respectively. Similar to olivine, pyroxene in the gabbro has a narrow magnesium number range (Mg#=71–80).

Olivine and feldspar contain almost no titanium and the pyroxene has a Ti content of less than 1%. The NWA 6950 minerals have very low titanium (VLT) in concentration.

3.2 U-Pb chronology of baddeleyite and phosphate

Zircons are not found in NWA 6950 but many anhedral baddeleyite grains occur. Their grain size is mostly between 3 μm and 15 μm and the grains rims are usually elongate and are usually associated with ilmenite, olivine, apatite, and merrillite. Nine baddeleyite grains are found on one thin slice (Figure 5(a1)–(a7)). Phosphate in lunar rocks is another U-bearing mineral available for dating [32, 34, 35]. The phosphates in NWA 6950 are mainly F-bearing apatite and merrillite. The amount of apatite is much larger than that of baddeleyite, and their size is mostly from several μm to 20 μm, with the biggest one being nearly 100 μm in length. Phosphates in the thin slice used for dating include 10 apatites and 2 merrillites (Figure 5(b1)–(b8)). Fifteen analyses are completed (2 and 3 spots are made on the largest two apatites respectively). The SHRIMP U-Pb results for the grains of baddeleyites and phosphates are shown in Table 2.

The phosphates (apatites and merrillites in Table 3) have an elongate skeletal morphology (Figure 2(b)) and occur alongside plagioclase and ilmenite, with occasional baddeleyite. The apatite is significantly enriched in fluorine, with values of 1–6 wt.%. Their FeO content is 0.2 wt.% to 0.8 wt.%, and the Cl content is about 0.05 wt.% to 0.2 wt.%. The content of Ce_2O_3 in merrillite is significantly higher than that of apatite. This is to be expected, as merrillite is richer than apatite in rare earth elements [25].

A functional relationship between $^{206}Pb^+/^{238}U^+$ and $^{254}[UO]^+/^{238}U^+$ has been used by different investigators on different minerals (zircon, baddeleyite, monazite and rutile) for Pb/U calibration of ion microprobe analyses [29]. This can be expressed using the following equation:

$$^{206}Pb^+/^{238}U^+ = A(^{254}[UO]^+/^{238}U^+)^E.$$

The equation has been widely used and well documented, where E is the exponent coefficient used

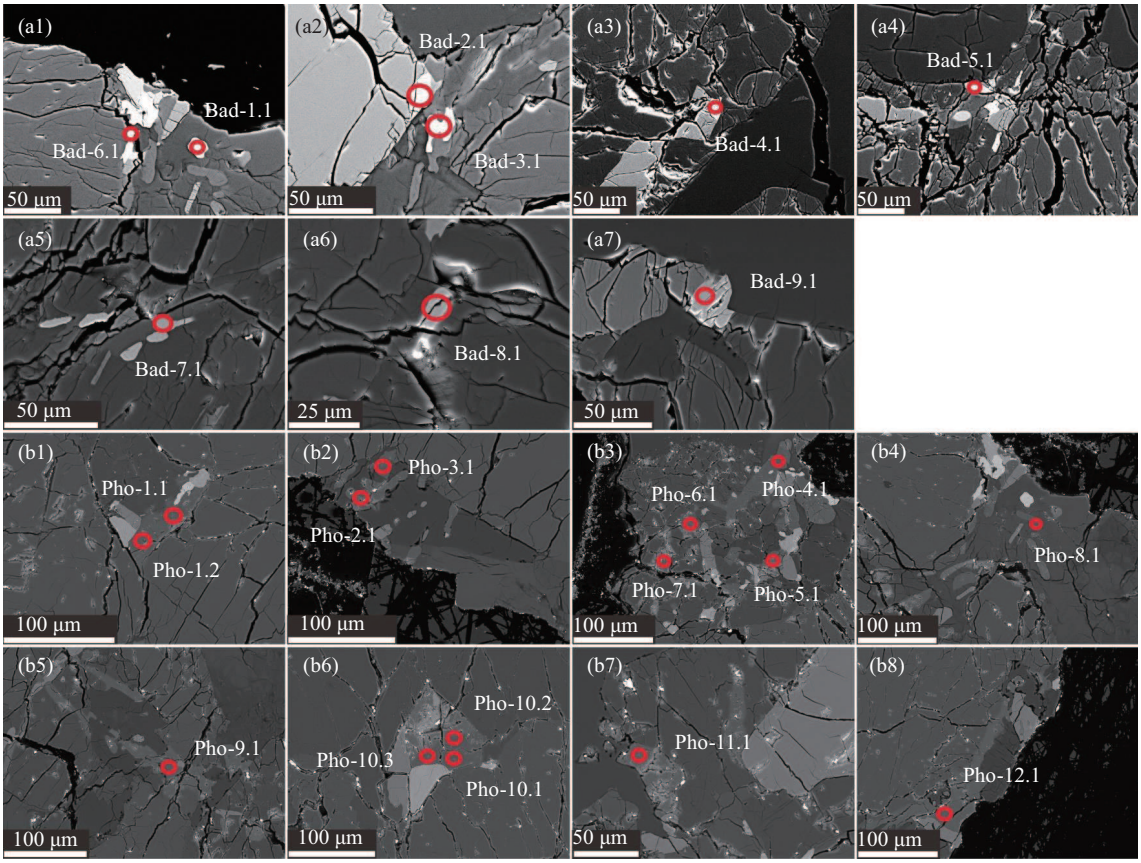

Figure 5 Secondary electron images of baddeleyites and phosphates used for U-Pb dating. (a1)–(a7) are images of baddeleyites; (b1)–(b8) are images of phosphates.

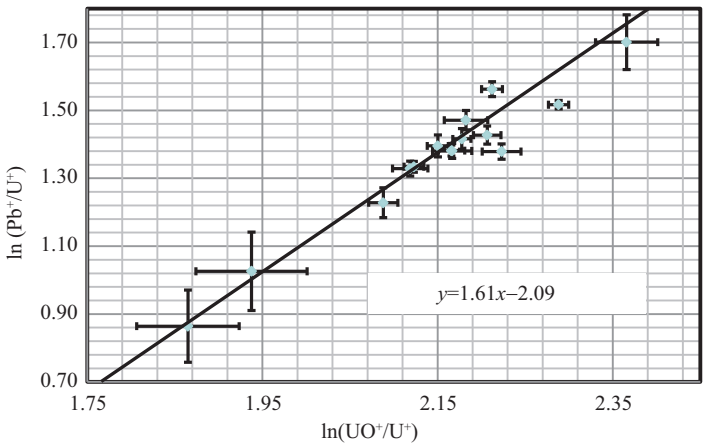

Figure 6 U-Pb calibration lines for SIMS analyses of phosphate.

for calibrating Pb/U against $^{254}[UO]^+/^{238}U^+$ for most minerals. But for apatite, there is no consensus on the value for E. It ranges from 1.26 to 1.94 [30, 32, 33] and is related to instrument characteristics and working status. Here, in order to increase the accuracy of the dating, we measured the value of E (Figure 6). For the Lunar thin slice sample in the mount in this time, E is 1.61, different from the value calculated in previous studies.

The weighted mean age of $^{207}Pb/^{206}Pb$ of baddeleyite is 3119 ± 16 Ma (Figure 6), MSWD = 2.5 (mean squared weighted deviates, MSWD), which is slightly higher than the previous analysis of the same sample ((3100 ± 16) Ma, [4]). The weighted mean age of $^{207}Pb/^{206}Pb$ of phosphate is (3119 ± 18) Ma (MSWD = 2.1, Figure 7), which is the same as baddeleyite. By comparing these ages with the crystallization ages

Table 2 SHRIMP U-Pb data for the grains of baddeleyite and phosphate

Sample	Spots#	U (ppm)	Th (ppm)	Pb (ppm)	$^{232}Th/^{238}U$	$^{206}Pb/^{238}U$	$\pm\sigma$ (%)	$^{207}Pb/^{206}Pb$	$\pm\sigma$ (%)	$^{207}Pb/^{235}U$	$\pm\sigma$ (%)	$^{206}Pb/^{238}U$ (Ma)	$\pm\sigma$ (Ma)	$^{207}Pb/^{206}Pb$ (Ma)	$\pm\sigma$ (Ma)
Baddeleyite	Bad-1.1	93	8	50	0.09	0.6178	2.9	0.2405	1.1	20.48	3.1	3101	72	3123	18
	Bad-2.1	40	2	23	0.04	0.6608	2.9	0.2359	1.1	21.49	3.1	3270	75	3092	17
	Bad-3.1	60	5	34	0.09	0.6498	2.9	0.2407	0.90	21.56	3.0	3227	73	3125	14
	Bad-4.1	247	14	140	0.06	0.6587	2.6	0.2399	0.42	21.79	2.7	3262	68	3120	7
	Bad-5.1	19	1	12	0.04	0.6973	3.9	0.2471	2.7	23.76	4.8	3410	100	3166	43
	Bad-6.1	84	13	49	0.16	0.6813	3.1	0.2473	1.1	23.23	3.3	3349	82	3168	17
	Bad-7.1	111	9	58	0.08	0.6102	2.7	0.2406	0.67	20.24	2.8	3071	66	3124	11
	Bad-8.1	151	6	86	0.04	0.6568	2.7	0.2349	0.85	21.27	2.9	3255	70	3086	14
	Bad-9.1	16	0	8	0.03	0.5911	3.8	0.233	2.1	18.99	4.3	2994	90	3073	34
Phosphate	Pho-1.1	63	159	30	2.6	0.5613	5.0	0.2451	2.4	18.97	5.5	2872	120	3153	37
	Pho-1.2	98	216	48	2.3	0.5690	4.8	0.2434	1.3	19.10	5.0	2904	110	3143	21
	Pho-2.1	125	213	59	1.8	0.5501	4.8	0.2441	1.7	18.51	5.1	2826	110	3147	27
	Pho-3.1	143	228	70	1.6	0.5680	4.8	0.2424	1.5	18.98	5.0	2899	110	3136	24
	Pho-4.1	102	351	51	3.6	0.5869	4.8	0.2398	1.4	19.41	5.0	2977	110	3119	23
	Pho-5.1	95	437	49	4.8	0.5955	4.8	0.2382	1.5	19.56	5.0	3012	110	3108	24
	Pho-6.1	68	290	35	4.4	0.5994	5.0	0.2456	3.1	20.30	5.9	3028	120	3156	49
	Pho-7.1	73	283	35	4.0	0.5513	5.0	0.2375	3.1	18.06	5.9	2831	110	3103	50
	Pho-8.1	79	181	38	2.4	0.5679	4.8	0.2508	2	19.64	5.2	2899	110	3190	31
	Pho-9.1	84	147	46	1.8	0.6490	4.8	0.2484	1.4	22.23	5.0	3224	120	3174	23
	Pho-10.1	203	64	103	0.3	0.5914	4.8	0.2360	0.94	19.24	4.8	2995	110	3093	15
	Pho-10.2	159	78	82	0.5	0.5982	4.7	0.2336	1.1	19.27	4.8	3023	110	3077	17
	Pho-10.3	171	62	89	0.4	0.6036	4.7	0.2358	1.2	19.62	4.9	3044	110	3092	20
	Pho-11.1	163	677	78	4.3	0.5598	4.7	0.2422	0.95	18.70	4.8	2866	110	3135	15
	Pho-12.1	135	292	75	2.2	0.6475	4.8	0.2358	1.3	21.05	5.0	3218	120	3092	20

Table 3 Compositions of major elements of phosphate from NWA 6950[a)]

Phosphate (wt.%)	Pho-1	Pho-2	Pho-3	Pho-4	Pho-5	Pho-6	Pho-7	Pho-8	Pho-9	Pho-10	Pho-11	Pho-12
	Apa	Apa	Apa	Apa	Mrl	Apa	Apa	Apa	Apa	Apa	Mrl	Apa
P_2O_5	42.78	40.68	41.82	41.43	44.86	40.10	41.16	42.26	40.64	42.02	44.97	40.69
CaO	51.67	54.15	54.56	54.22	45.07	53.64	53.20	55.48	54.03	54.71	45.18	53.75
MgO	1.91	0.15	0.06	0.11	3.50	0.13	0.42	0.00	0.12	0.12	3.51	0.39
F	1.08	3.57	2.58	4.29	0.10	3.60	5.80	3.32	3.01	3.83	0.32	3.51
Cl	0.14	0.14	0.15	0.18	bd	0.17	0.26	0.06	0.88	0.08	bd	0.23
FeO	1.09	0.60	0.60	0.36	0.74	0.35	0.67	0.19	0.54	0.65	0.81	0.79
MnO	0.05	0.02	bd	bd	bd	0.03	bd	0.08	0.03	bd	0.02	bd
Na_2O	0.19	0.01	0.06	0.02	0.44	bd	0.01	bd	0.01	bd	0.43	bd
SrO	bd	0.08	bd	bd	0.02	bd	bd	0.01	bd	0.06	0.07	0.07
La_2O_3	bd	bd	bd	0.06	0.19	0.06	bd	0.02	bd	0.01	bd	bd
Ce_2O_3	0.39	0.27	0.13	0.29	0.54	0.31	0.47	0.04	0.36	0.12	0.97	0.28
Total	99.30	99.67	99.97	100.96	95.46	98.38	101.98	101.43	99.62	101.60	96.28	99.71

a) Apa: Apatite; Mrl: merrillite; bd: below detection limit.

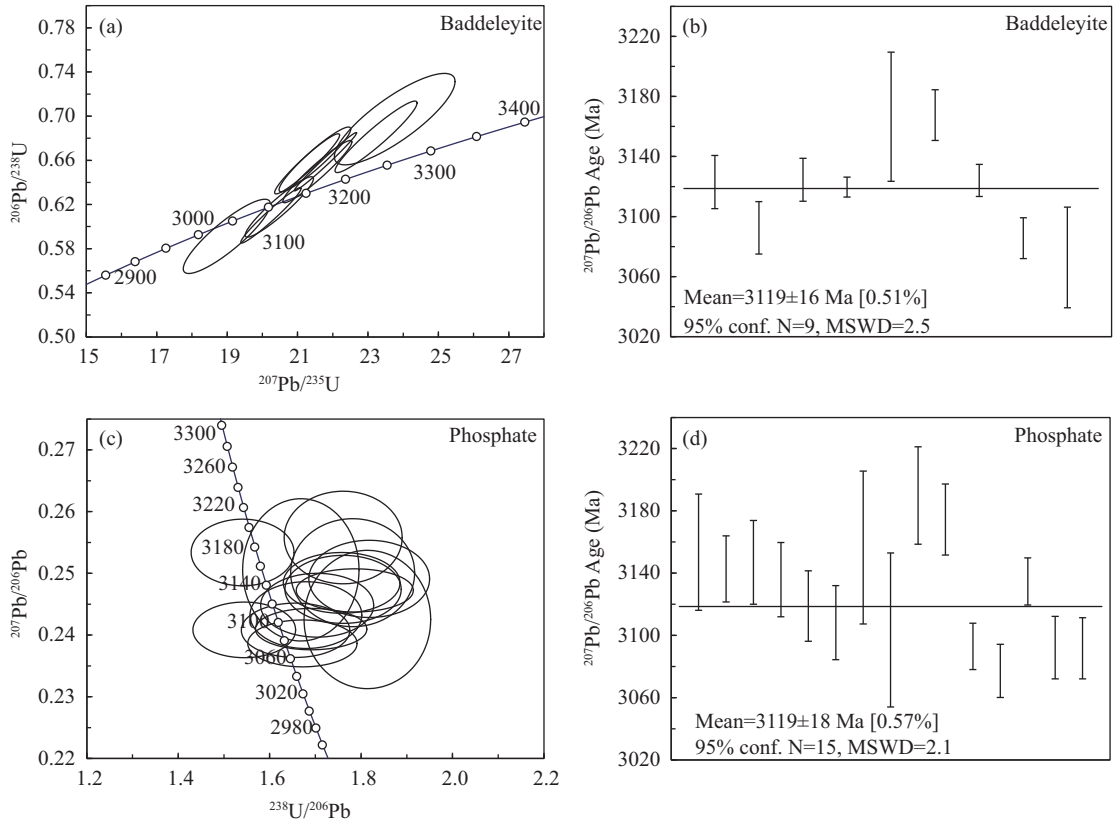

Figure 7 U-Pb concordia and $^{207}Pb/^{206}Pb$ weighted average dates of phosphate and baddeleyite determined by SHRIMP II.

of the gabbro lithology of NWA 773 clan of meteorites (Table 4 [4, 5, 17, 18, 24, 25, 36]), it is concluded that the age of NWA 6950 is nearly the same.

4 Discussion

The petrological and mineralogical characteristics of the Lunar meteorite NWA 6950 are identical to the magnesian gabbro part of NWA 773. The lithologies of NWA 773 and its paired meteorites include magnesian gabbro, ferroan gabbro, anorthositic gabbro, olivine phyric basalt and regolith breccia [37]. NWA

Table 4 Summary of isotopic ages (in Ma) of NWA 773 and its paired lunar meteorites[a)]

Sample	Age (Ma)	Method	Material	Ref.
NWA 773	3129±11 (95% conf.)	Pb-Pb	baddeleyite	[5]
	2865±31 (2σ)	Sm-Nd	Whole rock	[18]
	2670±10 (2σ)	Ar-Ar	Whole rock	[17]
NWA 3160	2650±40 (2σ)	Ar-Ar	Whole rock	[36]
NWA 3170	3118±14 (95% conf.)	Pb-Pb	baddeleyite	[5]
NWA 7007	3106±22 (95% conf.)	Pb-Pb	baddeleyite	[5]
NWA 6950	3100±16 (95% conf.)	Pb-Pb	baddeleyite	[4]
	3119±18 (95% conf.)	Pb-Pb	phosphate	This study
	3119±16 (95% conf.)	Pb-Pb	baddeleyite	This study
NWA 2977	3123±7 (2σ)	Pb-Pb	baddeleyite	[25]
	3100±50 (2σ)	Sm-Nd	Whole rock	[24]
	3290±110 (2σ)	Rb-Sr	Whole rock	[24]

a) 95% conf.: the uncertainties are cited at the 95% confidence limit.

6950 has a simple magnesian gabbro lithology and is rich in olivine, pyroxene and vitreous plagioclase. Augite and pigeonite have narrow compositional ranges of $En_{46\text{-}52}Fs_{12\text{-}16}Wo_{32\text{-}41}$ and $En_{58\text{-}68}Fs_{19\text{-}28}Wo_{7\text{-}20}$ (Table 1), respectively. The olivine of NWA 6950 and NWA 773 is likewise similar in term of Mg/Fe ratio, Ca and Mn. The plagioclase crystal's form and its Na, K, Fe contents are the same for the NWA 773 meteorites [5, 25]. We conclude that NWA 6950 is texturally and mineralogically identical to the olivine gabbro clasts in the NWA 773 meteorite clan and that there is a connection in their source of origin and formation.

The crystallization sequence of these lithologies cannot be separated by the reported chronological data. However, according to the Mg of the pyroxene in various lithologies, Valencia et al. [37] inferred that the magnesian gabbro crystallized first, and then anorthositic gabbro, and the last to crystallize was ferroan gabbro. The U concentration in baddeleyite and the U, Th, Ce contents in phosphate are at high levels (Tables 2 and 3), which both indicate there are high concentrations of incompatible elements in NWA 6950. Zhang et al. [25] found that the same enrichment exists in NWA 2977.

The baddeleyite and phosphate $^{207}Pb/^{206}Pb$ crystallization ages are identical in NWA 6950. Moreover, both are similar to some NWA 773 paired meteorites [5, 25]. Considering the successive discovery of a multiple of NWA 773 clan of meteorites, it is inferred that there is magmatic activity in the KREEP region of the Moon at about 3.12 billion years ago and that various rocks with different lithologies such as magnesian gabbro, ferroan gabbro and anorthositic gabbro are formed [5]. The parent magma for the meteorites has been suggested to be similar to an Apollo 14 VLT picritic glass [38], with an addition, possibly by assimilation of or mixing in the source region with a KREEP-rich component [24, 25]. There are more than 30 lunar basalts that younger than 3400 Ma (Figure 8 [3–5, 14, 15, 18, 25, 39, 40]). In general, the formation of high Ti basalts on the Moon occurs earlier than low Ti basalts. The Apollo missions obtain a large number of basalt samples and many low Ti basalts are from the Apollo12 and Apollo15 sites. The youngest lunar magma crystallization ages are measured in lunar meteorites [3, 17–19] in contrast to those obtained from Apollo missions samples.

The isotopic ages of NWA 773 and its paired lunar meteorites obtained by different methods (Table 4) span from 2650 Ma to 3290 Ma. The ages obtained by Ar-Ar are significantly younger than those obtained by Pb-Pb, Rb-Sr and Sm-Nd. The Pb-Pb age is the result of the two isotopic systems of ^{238}U-^{206}Pb and ^{235}U-^{207}Pb in the same mineral. Baddeleyite and phosphate are less susceptible to shock metamorphism than silicate minerals used for Ar-Ar and Sm-Nd dating, making the measured Pb-Pb dates more likely to reflect the crystallization age. The NWA 6950 measured by Shaulis et al. [4] is relatively younger than several other NWA 773 paired meteorites which may be related to the use of only four baddeleyites. However, in this study, two kinds of U-bearing minerals in the meteorite have an identical age. We consider that the ∼3119 Ma age is more accurate and reliable, reflecting crystallization age of the meteorite.

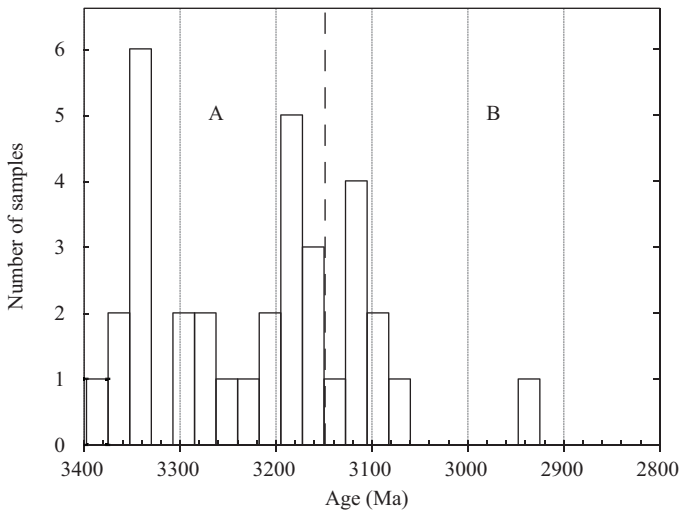

Figure 8 Crystallization age for more than 30 lunar igneous stones that are younger than 3400 Ma. Section A: crystallization ages from basalts from Apollo12 and Apollo15 [14,15,39,40]. Section B: crystallization ages of young lunar igneous meteorite [3–5,18,25].

A 2.6 Ga Ar-Ar crystallization age is measured for NWA 773 [17,36]. From the technical details, a 3 mm diameter laser beam for sample heating was used in that study. Perhaps the single-point analytical area includes a mix of olivine, pyroxene, and plagioclase. Considering the late-stage high-intensity shock metamorphism, combined with the mineralogical characteristics of our sample, the rock mass may have been impacted at 2.6 Ga, and the radiogenic Ar evaporated causing the age to be reset or partially reset [25].

The Apollo12 landing site is located in the south of Oceanus Procellarum area and is the youngest of all Apollo missions. Almost every reported isotopic age younger than 3.2 Ga comes from the Apollo 12 samples ([39], and references therein). Rb-Sr age of basalt samples 12051, 12065, are as young as ∼3160 Ma [14,15], which is close to the age obtained for NWA 6950. Considering the geochemical characteristic of a KREEP component incorporation [25,38], we suggest that Procellarum KREEP Terrane (PKT) may have been a potential material source of NWA 6950. This would then indicate that there is magmatic activity in the KREEP region at ca. 3119 Ma.

5 Conclusion

The petrological and mineralogical analyses of lunar meteorite NWA 6950, combined with the identical U-Pb isotopic ages of its baddeleyite and phosphate, suggest that NWA 6950 has similar chemistry composition, geochemical characteristics, and age of crystallization to those of the magnesian gabbro of the NWA 773 clan. We concluded that NWA 6950 and NWA 773 are paired meteorites, which were formed at ca. 3119 Ma and they represent magmatism in the KREEP region of the Moon.

Acknowledgements This work was financially supported by National Nature Science Foundation of China (Grant Nos. 41842060, 41803027), China National Space Administration (Grant No. D020205), and China Geological Survey Research Fund (Grant Nos. JYYWF20180104, JYYWF20181702). We thank members of the Beijing SHRIMP Center for their help with SHRIMP analysis and sample imaging. We are also grateful to Prof. John W. VALLEY for his constructive comments for the paper.

References

1 Warren P H, Kallemeyn G W. Geochemical investigation of five lunar meteorites: implications for the composition, origin and evolution of the lunar crust. Proc NIPR Symp Antarcti Meteorites, 1991, 4: 91–117

2 Hsu W, Zhang A, Bartoschewitz R, et al. Petrography, mineralogy, and geochemistry of lunar meteorite Sayh al Uhaymir 300. Meteoritics Planet Sci, 2008, 43: 1363–1381

3 Wang Y, Hsu W, Guan Y, et al. Petrogenesis of the Northwest Africa 4734 basaltic lunar meteorite. GeoChim CosmoChim Acta, 2012, 92: 329–344
4 Shaulis B J, Righter M, Lapen T J, et al. Baddeleyite chronology of Northwest Africa 6950: A 3.1 Ga lunar olivine gabbro paired with NWA 2977 and the cumulate mare gabbro lithology in NWA 773. In: Proceedings of the 43rd Lunar and Planetary Science Conference, 2012. 2236
5 Shaulis B J, Righter M, Lapen T J, et al. 3.1 Ga crystallization age for magnesian and ferroan gabbro lithologies in the Northwest Africa 773 clan of lunar meteorites. Geochim Cosmochim Acta, 2017, 213: 435–456
6 Fagan T J, Taylor G J, Keil K, et al. Northwest Africa 773: lunar origin and iron-enrichment trend. Meteoritics Planet Sci, 2003, 38: 529–554
7 Bunch T E, Wittke J H, Korotev R L, et al. Lunar meteorites NWA 2700, NWA 2727 and NWA 2977: Mare basalt/gabbro brecciaswith affinities to NWA 773. In: Proceedings of the 37th Lunar and Planetary Science Conference, 2006. 1375
8 Zeigler R A, Korotev R L, Jolliff B L. Petrography, geochemistry, and pairing relationships of basaltic lunar meteorite stones NWA 773, NWA 2700, NWA 2727, NWA2977, and NWA 3160. In: Proceedings of the 38th Lunar and Planetary Science Conference, 2007. 2109
9 North S N, Jolliff B L, Korotev R L. Ferroan gabbro and leucogabbro lithologies in NWA 3170, possible petrogenetic link and comparison to NWA 2727. In: Proceedings of the 45th Lunar and Planetary Science Conference, 2014. 2858
10 Nagaoka H, Karouji Y, Takeda H. Mineralogy and petrology of lunarmeteorite Northwest Africa 2977 consisting of olivine cumulate gabbroincluding inverted pigeonite. Earth Planets Space, 2015, 67: 1–8
11 Yokoi N, Takenouchi A, Mikouchi T. Iron valencestates of plagioclase in some lunar meteorites. In: Proceedings of the 49th Lunar and Planetary Science Conference, 2018. 2227
12 Chen J, Jolliff B L, Korotev R L. Northwest Africa 10985: a new lunar gabbro? In: Proceedings of the 50th Lunar and Planetary Science Conference, 2019. 2132
13 Jolliff B L, Korotev R L, Zeigler R A, et al. Northwest Africa 773: lunar mare breccia with a shallow-formed olivine-cumulate component, inferred very-low-Ti (VLT) heritage, and a KREEP connection. Geochim Cosmochim Acta, 2003, 67: 4857–4879
14 Papanastassiou D A, Wasserburg G J. Lunar chronology and evolution from RbSr studies of Apollo 11 and 12 samples. Earth Planet Sci Lett, 1971, 11: 37–62
15 Nyquist L E, Bansal B M, Wooden J, et al. Sr-isotopic constraints on the peterogenesis of Apollo 12 mare basalts. In: Proceedings of the 8th Lunar and Planetary Science Conference, 1977. 1383–1415
16 OuYang Z. Introduction to Lunar Science (in Chinese). Beijing: Astronautic Publishing House, 2005
17 Fernandes V A, Burgess R, Turner G. ^{40}Ar-^{39}Ar chronology of lunar meteorites Northwest Africa 032 and 773. Meteoritics Planet Sci, 2003, 38: 555–564
18 Borg L E, Shearer C K, Asmerom Y, et al. Prolonged KREEP magmatism on the Moon indicated by the youngest dated lunar igneous rock. Nature, 2004, 432: 209–211
19 Rankenburg K, Brandon A D, Norman M D. A Rb Sr and Sm Nd isotope geochronology and trace element study of lunar meteorite LaPaz Icefield 02205. Geochim Cosmochim Acta, 2007, 71: 2120–2135
20 Shearer C K, Borg L E, Papike J J. A view of KREEP-rich lunar basaltic magmatism through the eyes of NWA 773. In: Proceedings of the 36th Lunar and Planetary Science Conference, 2005. 1191
21 Fagan T J, Kashima D, Wakabayashi Y, et al. Case study of magmatic differentiation trends on the Moon based on lunar meteorite Northwest Africa 773 and comparison with Apollo 15 quartz monzodiorite. Geochim Cosmochim Acta, 2014, 133: 97–127
22 Fagan T J, Nagaoka H. Northwest Africa 773 clan olivinecumulate gabbros: Crystallization trends compared with a gabbroic sill from Murotomisaki. In: Proceedings of the 80th Annual Meeting of the Meteoritical Society, 2017. 6082
23 Kayama M, Tomioka N, Ohtani E, et al. Discovery of moganite in a lunar meteorite as a trace of H2O ice in the Moon's regolith. Sci Adv, 2018, 4: 4378
24 Nyquist L E, Shih C Y, Reese Y D, et al. Sm-Nd and Rb-Sr ages and isotopic systematic for NWA 2977, a young basalt from the PKT. Meteorit Planet Sci, 2009, 44: 159
25 Zhang A, Hsu W, Floss C, et al. Petrogenesis of lunar meteorite northwest Africa 2977: constraints from in-situ microprobe results. Meteorit Planet Sci, 2011, 45: 1929–1947
26 Borg L E, Gaffney A M, Shearer C K, et al. Mechanisms for incompatible-element enrichment on the Moon deduced from the lunar basaltic meteorite Northwest Africa 032. Geochim Cosmochim Acta, 2009, 73: 3963–3980
27 Ruzicka A, Grossman J N, Garvie L. The Meteoritical Bulletin, No. 100, 2014 June. Meteorit Planet Sci, 2014, 49: 1–101
28 Heaman L M. The application of U-Pb geochronology to mafic, ultramafic and alkaline rocks: an evaluation of three mineral standards. Chem Geol, 2009, 261: 43–52
29 Williams I S. U-Th-Pb geochronology by ion microprobe. Rev Economic Geology, 1998, 7: 1–35
30 Li Q L, Li X H, Wu F Y, et al. In-situ SIMS U-Pb dating of phanerozoic apatite with low U and high common Pb. Gondwana Res, 2012, 21: 745–756
31 Trotter J A, Eggins S M. Chemical systematics of conodont apatite determined by laser ablation ICPMS. Chem Geol, 2006, 233: 196–216
32 Nemchin A A, Pidgeon R T, Healy D, et al. The comparative behavior of apatite-zircon U-Pb systems in Apollo 14 breccias: implications for the thermal history of the Fra Mauro Formation. Meteoritics Planet Sci, 2009, 44: 1717–1734
33 Sano Y, Oyama T, Terada K, et al. Ion microprobe U-Pb dating of apatite. Chem Geol, 1999, 153: 249–258

34 Lin Y, Shen W, Liu Y, et al. Very high-K KREEP-rich clasts in the impact melt breccia of the lunar meteorite SaU 169: new constraints on the last residue of the Lunar Magma Ocean. Geochim Cosmochim Acta, 2012, 85: 19–40
35 Wu Y, Hsu W. Mineral chemistry and in-situ Usbnd Pb geochronology of the mare basalt Northwest Africa 10597: implications for low-Ti mare volcanism around 3.0 Ga. Icarus, 2020, 338: 113531
36 Burgess R, Fernandes V A, Irving A J, et al. Ar-Ar ages of nwa 2977 and NWA 3160–lunar meteorites paired with NWA 773. In: Proceedings of the 38th Lunar and Planetary Science Conference, 2007. 1603
37 Valencia S N, Jolliff B L, Korotev R L. Petrography, relationships, and petrogenesis of the gabbroic lithologies in Northwest Africa 773 clan members Northwest Africa 773, 2727, 3160, 3170, 7007, and 10656. Meteorit Planet Sci, 2019, 54: 2083–2115
38 Jolliff B L, Zeigler R A, Korotev R L. Compositional characteristics and petrogenetic relationships among the NWA 773 clan of lunar meteorites. In: Proceedings of the 38th Lunar and Planetary Science Conference, 2007. 1489
39 Meyer C. Lunar sample compendium. 2012. http://curator.jsc.nasa.gov/lunar/compendium.cfm
40 Papanastassiou D A, Wasserburg G J. RbSr ages and initial strontium in basalts from Apollo 15. Earth Planet Sci Lett, 1973, 17: 324–337